International Journal of Occupational Safety and Ergonomics (*JOSE*) 2007, Vol. 13, No. 2, 147–157

The Modal Low Frequency Noise of an Elastically Supported Circular Plate

Wojciech P. Rdzanek
Witold J. Rdzanek

Department of Acoustics, University of Rzeszów, Rzeszów, Poland

Zbigniew Engel

Department of Mechanics and Vibroacoustics, AGH University of Science and Technology, Kraków, Poland

Krzysztof Szemela

Department of Acoustics, University of Rzeszów, Rzeszów, Poland

The modal low frequency noise generated by a vibrating elastically supported circular plate embedded into a flat infinite baffle has been examined. The main aim of this study is the analysis of the radiation efficiency. Low frequency approximated formulas have been presented. They are valid for all the limiting boundary conditions of the plate with its edge clamped, guided, simply supported or free as well as for all the intermediate axisymmetric boundary configurations. The formulas are expressed in the elementary form, useful for numerical computations. They are a generalization of some earlier published results. First, they are valid for axisymmetric and asymmetric modes since both kinds of modes play an important role in the low frequency range. Second, a single formula for the radiation efficiency, valid for all the axisymmetric boundary configurations, has been proposed. A numerical example for the sound power radiation has been given for some hatchway covers mounted on a ship deck.

low frequency noise radiation efficiency circular plate hatchway

1. INTRODUCTION

Thin flat circular plates often appear in communication, transport, military, industry and in devices in common use. Usually, they are excited and become sources of unwanted sound exposing humans to noise. Therefore, it is necessary to examine acoustic quantities such as the radiation efficiency of such sound sources. A number of authors used some approximate methods for computing the radiation efficiency of some flat plates [1, 2, 3, 4, 5]. A few studies attempted to find some approximate formulas for radiation efficiency of a clamped circular plate applying some complete solutions to the vibration phenomena [6, 7, 8, 9].

So far, to the best knowledge of these authors, no generalized modal low frequency formulas have been presented for an elastically supported circular plate. Developing a single formula valid for any axisymmetric boundary configuration of the plate for all the axisymmetric and asymmetric modes would be especially useful and therefore this is the main aim of this study.

Correspondence and requests for offprints should be sent to Wojciech P. Rdzanek, Department of Acoustics, University of Rzeszów, Al. Rejtana 16, 35-310 Rzeszów, Poland. E-mail: <wprdzank@univ.rzeszow.pl>.

2. GOVERNING EQUATIONS

A thin elastically supported circular plate is embedded into a rigid infinite baffle. Low fluid loading has been assumed and all the internal damping has been neglected. The plate deflections and thickness have been assumed to be small as compared with other dimensions of the plate. The equation of motion takes the form of

$$(k_{mn}^{-4}\nabla^4 - 1)\, W_{mn}(r,\varphi) = 0, \tag{1}$$

where W_{mn} (r, φ) is the mode shape of the mode (m, n); $r \in [0, a]$ is the radial variable; a is the plate radius; $\varphi \in [0, 2\pi]$ is the angular variable; $m = 0, 1, 2, \ldots, \infty$ and $n = 1, 2, 3, \ldots, \infty$ are the numbers of nodal diameters and nodal circles, respectively; $\nabla^2 = (\partial^2/\partial r^2) + r^{-1}(\partial/\partial r) + r^{-2}(\partial^2/\partial\varphi^2)$; $k_{mn}^4 = \omega_{mn}^2 \rho h / D_E$; ω_{mn} is the eigenfrequency; $D_E = Eh^3/[12(1 - \nu^2)]$ is the bending stiffness; ρ, h, E, ν are the plate density, thickness, Young modulus and Poisson ratio, respectively. The solution for Equation 1 is

$$W_{mn}(r,\varphi) = \begin{Bmatrix} \cos m\varphi \\ \sin m\varphi \end{Bmatrix} W_{mn}(r), \tag{2}$$

$$W_{mn}(r) = \mathrm{A}_{mn}\,[J_m(k_{mn}\, r) + \mathrm{C}_{mn}\, I_m(k_{mn}\, r)], \tag{3}$$

where J_m $(\bullet)$, I_m $(\bullet)$ are the mth order Bessel and modified Bessel functions, respectively; A_{mn}, C_{mn} are unknown constants [10, 11]. The orthogonality condition [10] is

$$\int_0^{2\pi}\int_0^a W_{mn}(r,\varphi) W_{pq}(r,\varphi) r dr d\varphi = \pi a^2 \delta_{mp}\delta_{nq}, \tag{4}$$

where δ_{mp} and δ_{nq} are the Kronecker deltas, and the following integral

$$\int_0^{2\pi} \begin{Bmatrix} \cos m\varphi_0 \\ \sin m\varphi_0 \end{Bmatrix} \begin{Bmatrix} \cos p\varphi_0 \\ \sin p\varphi_0 \end{Bmatrix} d\varphi_0 = \frac{2\pi}{\varepsilon_m}\delta_{mp},$$

has been used to obtain

$$A_{mn}^2 = \frac{\varepsilon_m}{N_{mn}}, \qquad \varepsilon_m = \begin{cases} 1 & \text{for} \quad m = 0 \\ 2 & \text{for} \quad m > 0 \end{cases}, \tag{5}$$

$$\begin{aligned} N_{mn} &= \frac{2}{a^2}\int_0^a [J_m(k_{mn}r) + C_{mn} I_m(k_{mn}r)]^2 r dr \\ &= J_m^2(\lambda_{mn}) + J_{m+1}^2(\lambda_{mn}) - \frac{2m}{\lambda_{mn}} J_{m+1}(\lambda_{mn}) J_m(\lambda_{mn}) \\ &+ C_{mn}^2 \left[I_m^2(\lambda_{mn}) - I_{m+1}^2(\lambda_{mn}) - \frac{2m}{\lambda_{mn}} I_{m+1}(\lambda_{mn}) I_m(\lambda_{mn}) \right] \\ &+ \frac{2C_{mn}}{\lambda_{mn}} \left[J_{m+1}(\lambda_{mn}) I_m(\lambda_{mn}) + J_m(\lambda_{mn}) I_{m+1}(\lambda_{mn}) \right], \end{aligned} \tag{6}$$

where $\lambda_{mn} = k_{mn}\, a$ is the eigenvalue.

The plate satisfies uniform boundary conditions

$$V(a, \varphi) = - K_W W_{mn}(a, \varphi), \tag{7}$$

$$M(a,\varphi) = K_\psi \frac{\partial}{\partial r} W(r,\varphi)\Big|_{r=a}, \tag{8}$$

where K_W and K_ψ are the boundary stiffness values associated with the force V resisting transverse deflection of the plate edge and with the bending moment M of the edge, respectively [12]. The shearing force and the radial co-ordinate of the bending moment related to the length unity can be formulated as

$$V(r,\varphi) = -D_E \left[\frac{\partial}{\partial r}\nabla^2 + \frac{1-\nu}{r}\frac{\partial}{\partial r}\left(\frac{1}{r}\frac{\partial^2}{\partial\varphi^2} \right) \right] W_{mn}(r,\varphi)$$

and (9)

$$M(r,\varphi) = -D_E \left[\frac{\partial^2}{\partial r^2} + \frac{\nu}{r}\left(\frac{\partial}{\partial r} + \frac{1}{r}\frac{\partial^2}{\partial\varphi^2} \right) \right] W_{mn}(r,\varphi), \tag{10}$$

respectively. Inserting Equation 2 into Equations 7 and 8 gives the frequency equation

$$\begin{aligned} C_{mn} &= -\frac{\{m^2[(m-1)\nu+1] - q - m\lambda_{mn}^2\} J_m(\lambda_{mn}) + \lambda_{mn}(\lambda_{mn}^2 - m^2\nu) J_{m+1}(\lambda_{mn})}{\{m^2[(m-1)\nu+1] - q + m\lambda_{mn}^2\} I_m(\lambda_{mn}) + \lambda_{mn}(\lambda_{mn}^2 + m^2\nu) I_{m+1}(\lambda_{mn})} \\ &= \frac{\{\lambda_{mn}^2 - m[p + (m-1)(1-\nu)]\} J_m(\lambda_{mn}) + \lambda_{mn}(p + \nu - 1) J_{m+1}(\lambda_{mn})}{\{\lambda_{mn}^2 + m[p + (m-1)(1-\nu)]\} I_m(\lambda_{mn}) + \lambda_{mn}(p + \nu - 1) I_{m+1}(\lambda_{mn})}, \end{aligned} \tag{11}$$

where $q = K_W\, a^3/D_E$ and $p = K_\psi\, a/D_E$ are the dimensionless boundary stiffness values.

The Green function of the Neumann boundary value problem can be formulated as the Fourier series with respect to the angle variable φ:

$$G(r,\varphi,z\mid r_0,\varphi_0,0)=\sum_{s=0}^{\infty}\varepsilon_s\cos s(\varphi-\varphi_0)g_s(r,z\mid r_0,0), \quad (12)$$

where ε_s has been defined in Equation 5, the Fourier coefficients have been expressed in their Hankel representations [13, 14]

$$g_s(r,z\mid r_0,0)=\frac{i}{2\pi}\int_0^{\infty}e^{i\gamma z}J_s(\tau r)J_s(\tau r_0)\frac{\tau d\tau}{\gamma}, \quad (13)$$

and $\gamma=\sqrt{k^2-\tau^2}$; k is the acoustic wavenumber; $\tau=k\sin\vartheta$; $i=\sqrt{-1}$; (r, φ, z) are the polar co-ordinates of the field point; $(r_0, \varphi_0, 0)$ are the polar co-ordinates of the plate point; $r\in[0, a]$; $\varphi_0\in[0, 2\pi]$. The Fouries series for the Green's functions $G(\vec{r}\mid\vec{r}_0)=\sum^{+\infty}\exp[is(\varphi-\varphi_0)]g_s(r,z\mid r_0,0)$ has been substituted by that in Equation 12 since $J_{-s}(\tau r)J_{-s}(\tau r_0)=(-)^sJ_s(\tau r)(-)^sJ_s(\tau r_0)$. The origin of the co-ordinate system has been located in the plate center. The acoustic potential amplitude related to the mode (m, n) is

$$\phi_{mn}(r,\varphi,z)=\int_0^{2\pi}\int_0^{a}v_{mn}(r_0,\varphi_0)G(r,\varphi,z\mid r_0,\varphi_0,0)r_0dr_0d\varphi_0$$

$$=\sum_{s=0}^{\infty}\frac{\varepsilon_s}{2\pi}\omega_{mn}\begin{Bmatrix}\cos s\varphi\\ \sin s\varphi\end{Bmatrix}\int_0^{2\pi}\begin{Bmatrix}\cos m\varphi_0\\ \sin m\varphi_0\end{Bmatrix}\begin{Bmatrix}\cos s\varphi_0\\ \sin s\varphi_0\end{Bmatrix}d\varphi_0$$

$$\times\int_0^{\infty}e^{i\gamma z}J_s(\tau r)\int_0^{a}W_{mn}(r_0)J_s(\tau r_0)r_0dr_0\frac{\tau d\tau}{\gamma}, \quad (14)$$

where $v_{mn}(r, \varphi, t)=-i\omega_{mn}W_{mn}(r, \varphi)e^{-i\omega_{mn}t}$ is the modal vibration velocity function and t is the time variable. The sound pressure related to the mode (m, n) is

$$p_{mn}(r,\varphi,z)=-i\omega\rho_0\phi_{mn}(r,\varphi,z)$$

$$=-i\rho_0\omega\omega_{mn}\begin{Bmatrix}\cos m\varphi\\ \sin m\varphi\end{Bmatrix}\int_0^{\infty}e^{i\gamma z}J_m(\tau r)M_{mn}(\tau)\frac{\tau d\tau}{\gamma}, \quad (15)$$

where ρ_0 is the density of light fluid, ω is the circular frequency, and

$$M_{mn}(\tau)=\int_0^{a}W_{mn}(r_0)J_m(\tau r_0)r_0dr_0. \quad (16)$$

The radiation sound power related to the mode (m, n) can be formulated as

$$\Pi_{mn}=\frac{1}{2}\int_0^{2\pi}\int_0^{a}p_{mn}(r,\varphi,0)v_{mn}^{*}(r,\varphi)rdrd\varphi, \quad (17)$$

where $v_{mn}^{*}(r,\varphi)=i\omega_{mn}W_{mn}(r,\varphi)$ for some time-harmonic processes. The impedance approach requires that integrating be performed closely to the plate surface, i.e., for $z = +0$. Using Equation 17 and variable exchange $\tau=k\sin\vartheta$ leads to

$$\mathrm{Re}\Pi_{mn}=\frac{\pi}{\varepsilon_m}\rho_0c\omega_{mn}^2k^2\int_0^{\pi/2}M_{mn}^2(\vartheta)\sin\vartheta d\vartheta, \quad (18)$$

where k and c are the acoustic wavelength and sound velocity in fluid, respectively, and

$$M_{mn}(\vartheta)=\int_0^{a}W_{mn}(r)J_m(kr\sin\vartheta)rdr=2A_{mn}a^2\frac{\psi_{mn}(\vartheta)}{\lambda_{mn}}$$

$$\psi_{mn}(\vartheta)=\frac{J_{m+1}(\lambda_{mn})J_m(u)-u_{mn}J_m(\lambda_{mn})J_{m+1}(u)}{1-u_{mn}^4}$$

$$-\frac{d_{mn}J_m(u)-u_{mn}b_{mn}J_{m+1}(u)}{2(1+u_{mn}^2)} \quad (19)$$

$$u=\tau a,\ u_{mn}=\frac{\tau}{k_{mn}},$$

$$d_{mn}=J_{m+1}(\lambda_{mn})-C_{mn}I_{m+1}(\lambda_{mn}),$$

$$b_{mn}=J_m(\lambda_{mn})+C_{mn}I_m(\lambda_{mn}).$$

The reference sound power related to the mode (m, n) has been obtained using the facts that $\lim_{k\to\infty}p_{mn}=\rho_0cv_{mn}$ and $\int_0^{a}W_{mn}^2(r)rdr=\varepsilon_m a^2/2$ and (cf. Equations 5 and 6):

$$\Pi_{mn}^{(\infty)}=\lim_{k\to\infty}\Pi_{mn}=\frac{\rho_0c}{2}\int_0^{2\pi}\int_0^{a}v_{mn}^{*}(r,\varphi)rdrd\varphi=\frac{\rho_0c}{2}\pi a^2\omega_{mn}^2. \quad (20)$$

The radiation efficiency related to the mode (m, n) in its Hankel representation is

$$\sigma_{mn}=\mathrm{Re}\frac{\Pi_{mn}}{\Pi_{mn}^{(\infty)}}=q_{mn}^2\int_0^{\pi/2}\psi_{mn}^2(\vartheta)\sin\vartheta d\vartheta \quad (21)$$

where $q_{mn}=2\sqrt{2/\varepsilon_m}A_{mn}k/k_{mn}$.

3. LOW FREQUENCY APPROXIMATION

Using Equations 19 and 21 makes it possible to express radiation efficiency as

$$\sigma_{mn}=q_{mn}^2[\sigma_{mn}^{(1)}+\sigma_{mn}^{(2)}+\sigma_{mn}^{(3)}], \quad (22)$$

where

$$\sigma_{mn}^{(1)}=\int_0^{\pi/2}\left[\frac{J_{m+1}(\lambda_{mn})J_m(u)-u_{mn}J_m(\lambda_{mn})J_{m+1}(u)}{1-u_{mn}^4}\right]^2\sin\vartheta d\vartheta, \quad (23)$$

$$\sigma_{mn}^{(2)} = -\int_0^{\pi/2} \frac{J_{m+1}(\lambda_{mn})J_m(u) - u_{mn}J_m(\lambda_{mn})J_{m+1}(u)}{1-u_{mn}^4} \cdot \frac{d_{mn}J_m(u) - u_{mn}b_{mn}J_{m+1}(u)}{1+u_{mn}^2} \sin\vartheta\, d\vartheta, \tag{24}$$

$$\sigma_{mn}^{(3)} = \frac{1}{4}\int_0^{\pi/2} \left[\frac{d_{mn}J_m(u) - u_{mn}b_{mn}J_{m+1}(u)}{1+u_{mn}^2} \right]^2 \sin\vartheta d\vartheta. \tag{25}$$

Further, the following expansion series have been used

$$\frac{1}{(1-u_{mn}^4)^2} = 1 + 2u_{mn}^4 + O(u_{mn}^8), \tag{26}$$

$$\frac{1}{(1-u_{mn}^4)(1+u_{mn}^2)} = 1 - u_{mn}^2 + 2u_{mn}^4 - 2u_{mn}^6 + O(u_{mn}^8), \tag{27}$$

$$\frac{1}{(1+u_{mn}^2)^2} = 1 - 2u_{mn}^2 + 3u_{mn}^4 - 4u_{mn}^6 + O(u_{mn}^8), \tag{28}$$

where O (•) is the approximation error order. These expansion series are fast convergent within the integration limits in Equations 23–25. Inserting them into Equation 22 leads to

$$\sigma_{mn} = q_{mn}^2 \left\{ \sum_{l=1}^{4} (k/k_{mn})^{2l-2} \left[\hat{A}_l I_{A,l}^{(m)} + (k/k_{mn})\hat{B}_l I_{B,l}^{(m)} + (k/k_{mn})^2 \hat{C}_l I_{A,l}^{(m+1)} \right] + O\left[(k/k_{mn})^8 \right] \right\}, \tag{29}$$

where

$$\begin{aligned} \hat{A}_1 &= \left[J_{m+1}(\lambda_{mn}) - d_{mn}/2 \right]^2, \\ \hat{A}_2 &= d_{mn}\left[J_{m+1}(\lambda_{mn}) - d_{mn}/2 \right], \\ \hat{A}_3 &= (d_{mn}/2)^2 + 2\hat{A}_1, \quad \hat{A}_4 = 2\hat{A}_2, \end{aligned} \tag{30}$$

$$\begin{aligned} \hat{B}_1 &= -2\left[J_m(\lambda_{mn}) - b_{mn}/2 \right] \cdot \left[J_{m+1}(\lambda_{mn}) - d_{mn}/2 \right], \\ \hat{B}_2 &= d_{mn}b_{mn} - b_{mn}J_{m+1}(\lambda_{mn}) - d_{mn}J_m(\lambda_{mn}), \\ \hat{B}_3 &= 2\hat{B}_1 - d_{mn}b_{mn}/2, \quad \hat{B}_4 = 2\hat{B}_2, \end{aligned} \tag{31}$$

$$\hat{C}_1 = \left[J_m(\lambda_{mn}) - b_{mn}/2 \right]^2, \ \hat{C}_2 = b_{mn}\left[J_m(\lambda_{mn}) - b_{mn}/2 \right], \quad \hat{C}_3 = (b_{mn}/2)^2 + 2\hat{C}_1, \quad \hat{C}_4 = 2\hat{C}_2. \tag{32}$$

Using the following equations [11]

$$J_n(z)J_m(z) = \sum_{s=0}^{\infty} (-1)^s \frac{(n+m+2s)!\,(z/2)^{n+m+2s}}{s!\,(n+s)!\,(m+s)!\,(n+m+s)!}, \tag{33}$$

$$\int_0^{\pi/2} (\sin\vartheta)^{2l+1} d\vartheta = \frac{2^{2l}(l!)^2}{(2l+1)!}, \tag{34}$$

makes it possible to express the following integrals as their expansion series

$$I_{A,l}^{(m)} = \int_0^{\pi/2} (\sin\vartheta)^{2l-1} J_m^2(u) d\vartheta = \sum_{s=0}^{\infty} (-1)^s \frac{Z_{l,sm}(ka)^{2m+2s}}{s!\,(2m+s)!}, \tag{35}$$

$$I_{B,l}^{(m)} = \int_0^{\pi/2} (\sin\vartheta)^{2l} J_m(u)J_{m+1}(u) d\vartheta = \sum_{s=0}^{\infty} (-1)^s \frac{V_{l,sm}(ka)^{2m+2s+1}}{s!\,(2m+s+1)!}, \tag{36}$$

where

$$Z_{l,sm} = \begin{cases} \dfrac{1}{2m+2s+1} & \text{for} \quad l = 1 \\ \dfrac{2m+2s+2l-2}{2m+2s+2l-1} Z_{l-1,sm} & \text{for} \quad l > 1, \end{cases} \tag{37}$$

$$V_{l,sm} = \begin{cases} \dfrac{1}{2m+2s+3} & \text{for} \quad l = 1 \\ \dfrac{2m+2s+2l}{2m+2s+2l+1} V_{l-1,sm} & \text{for} \quad l > 1. \end{cases} \tag{38}$$

Further, the expansion series have been summed up introducing no additional error using the identity [11]

$$J_{2m}(2ka) = \sum_{s=0}^{\infty} (-1)^s \frac{(ka)^{2m+2s}}{s!\,(2m+s)!}, \tag{39}$$

which has given

$$\begin{cases} I_{A,1}^{(m)} = A_1, \quad I_{A,2}^{(m)} = A_1 + A_2, \\ 8I_{A,3}^{(m)} = 2A_2 + 3(A_1 + A_3) \\ 16I_{A,4}^{(m)} = 3(A_2 + A_3) + 5(A_1 + A_4), \end{cases} \tag{40}$$

$$\begin{cases} I_{B,1}^{(m)} = B_1, \quad I_{B,2}^{(m)} = B_1 + B_2, \\ 8I_{B,3}^{(m)} = 2B_2 + 3(B_1 + B_3) \\ 16I_{B,4}^{(m)} = 3(B_2 + B_3) + 5(B_1 + B_4), \end{cases} \tag{41}$$

where

$$A_l = \sum_{s=0}^{\infty} (-1)^s \frac{(ka)^{2m+2s}}{s!(2m+s)!(2m+2s+2l-1)} = \frac{1}{2ka} \begin{cases} \int_0^{2ka} J_{2m}(x)dx & \text{for} \quad l = 0 \\ J_{2m+1}(2ka) + (2m-2l+1)B_l & \text{for} \quad l > 0, \end{cases} \tag{42}$$

$$B_l = \sum_{s=0}^{\infty}(-1)^s \frac{(ka)^{2m+2s+1}}{s!(2m+s+1)!(2m+2s+2l+1)} = \frac{1}{2ka}[(2m+2l-1)A_l - J_{2m}(2ka)] \quad \text{for} \quad l>0. \tag{43}$$

The elementary value of the integral $\int_0^{2ka} J_{2m}(x)dx$ in Equation 42 for $l = 0$ can be obtained from the formulas

$$\int_0^{2ka} x^l J_{2m}(x)dx = \frac{-(2ka)^{l+1}J_{2m}(2ka) + \int_0^{2ka} x^{l+1}J_{2m-1}(x)dx}{2m-l-1}, \tag{44}$$

$$\int_0^{2ka} x^m J_m(x)dx = \frac{(2ka)^{m+1}J_m(2ka)}{2m+1} + 2^m(ka)\sqrt{\pi}\Gamma(m+1/2)\,[J_{m+1}(2ka)\boldsymbol{H}_m(2ka) - J_m(2ka)\boldsymbol{H}_{m+1}(2ka)], \tag{45}$$

where $l = 1, 2, 3, 4$, $m = 0, 1, 2, ..., \infty$, $\boldsymbol{H}_m$ is the mth order Struve function, and Γ is the Euler function [11]. Inserting Equations 30–32 and 40–41 into Equation 29 gives the low frequency approximation of the modal radiation efficiency of the plate.

4. THE TOTAL SOUND POWER

The formulas presented in section 3 for the modal radiation efficiency can be easily used to obtain the total sound power radiated by an excited plate. The following example has been considered. A hailstone strikes a circular hatchway cover. The cover is excited for some vibrations and becomes a sound source. The time-average sound power radiated depends on the excitation as well as on the plate material and geometric parameters. The acoustic and internal damping has been neglected for simplification. The equation of motion is

$$\left(k_D^{-4}\nabla^4 - 1\right)W(r,\varphi) = \frac{f(r,\varphi)}{\rho h\omega^2}, \tag{46}$$

where $k_D^4 = \omega^2\rho h/D$ is the structural wavenumber; $D = D_E(1 - i\omega\eta)$; $\eta \approx 0$, is the internal damping factor; ω is the excitation frequency; $f(r, \varphi)$ is the excitation amplitude distribution. The solution of Equation 46 can be expressed in the form of double infinite sums of eigenfunctions

$$W(r,\varphi) = \sum_{m=0}^{\infty}\sum_{n=1}^{\infty}\left[c_{mn}^{(c)}W_{mn}^{(c)}(r,\varphi) + c_{mn}^{(s)}W_{mn}^{(s)}(r,\varphi)\right], \tag{47}$$

where $W_{mn}^{(c)}(r,\varphi) = W_{mn}(r)\cos m\varphi$, $W_{mn}^{(s)}(r,\varphi) = W_{mn}(r)\sin m\varphi$ and

$$W_{mn}(r) = A_{mn}\left[J_m(k_{mn}r) + C_{mn}I_m(k_{mn}r)\right],$$
$$c_{mn}^{(\mu)} = \frac{f_{mn}^{(\mu)}}{(k_{mn}^4/k_D^4) - 1}, \tag{48}$$
$$f_{mn}^{(\mu)} = \frac{1}{\rho\omega^2 h\pi a^2}\int_0^{2\pi}\int_0^a f(r,\varphi)W_{mn}^{(\mu)}(r,\varphi)rdrd\varphi,$$

where $\mu \in \{c, s\}$. The intermodal sound power can be computed on the basis of Equations 15–17 and formulated as

$$\Pi_{mn,pq} = \frac{\rho_0\omega_{mn}\omega_{pq}\omega}{4\pi}\int_0^{\infty}\left(\sum_{s=0}^{\infty}\varepsilon_s\int_0^a W_{mn}(r)J_s(\tau r)rdr \times\int_0^a W_{pq}(r)J_s(\tau r)rdr\int_0^{2\pi}\begin{Bmatrix}\cos m\varphi_0\cos s\varphi_0\\ \sin m\varphi_0\sin s\varphi_0\end{Bmatrix}d\varphi_0 \times\int_0^{2\pi}\begin{Bmatrix}\cos p\varphi\cos s\varphi\\ \sin p\varphi\sin s\varphi\end{Bmatrix}d\varphi\right)\frac{\tau d\tau}{\sqrt{k^2-\tau^2}}. \tag{49}$$

Using the integral given after Equation 4 leads to

$$\Pi_{mn,mq} = \frac{\pi\rho_0\omega_{mn}\omega_{mq}\omega}{\varepsilon_m}\int_0^{\infty}M_{mn}(\tau)M_{mq}(\tau)\frac{\tau d\tau}{\sqrt{k^2-\tau^2}}. \tag{50}$$

Making use of Equations 19 and 20 the total sound power can be formulated as

$$\Pi = \sum_{m=0}^{\infty}\sum_{n=1}^{\infty}\sum_{q=1}^{\infty}\overline{c}_{mn,mq}^2\sqrt{\Pi_{mn}^{(\infty)}\Pi_{mq}^{(\infty)}}\,\sigma_{mn,mq}, \tag{51}$$

where the intermodal efficiency related to the modes (m, n) and (m, q) is

$$\sigma_{mn,mq} = \frac{\Pi_{mn,mq}}{\sqrt{\Pi_{mn}^{(\infty)}\Pi_{mq}^{(\infty)}}} = q_{mn}q_{mq} \times\int_0^{\pi/2}\psi_{mn}(\vartheta)\psi_{mq}(\vartheta)\sin\vartheta d\vartheta, \tag{52}$$

coefficients q_{mn} and q_{mq} have been defined after Equation 21,

$$\overline{c}_{mn,mq}^2 = c_{mn}^{(s)}c_{mq}^{(s)} + c_{mn}^{(c)}c_{mq}^{(c)}, \tag{53}$$

and the functions Ψ_{mn}, Ψ_{mq} are given by Equation 19. Using Equations 51, 52 and 48 makes it possible to calculate the total active sound power

for any asymmetric excitation. The excitation has been modeled by means the Dirac delta function

$$f(r,\varphi) = F_0 \frac{\delta(r-a_0)}{r}\delta(\varphi-\varphi_0), \tag{54}$$

where F_0 is the excitation amplitude, (a_0, φ_0) are the polar co-ordinates of the excitation force concentration. By employing Equation 48 the following is obtained:

$$\begin{aligned} c_{mn}^{(c)} &= \frac{F_0}{\pi\rho\omega^2 h a^2}\frac{W_{mn}(a_0)\cos m\varphi_0}{(k_{mn}/k_D)^4-1}, \\ c_{mn}^{(s)} &= \frac{F_0}{\pi\rho\omega^2 h a^2}\frac{W_{mn}(a_0)\sin m\varphi_0}{(k_{mn}/k_D)^4-1}, \end{aligned} \tag{55}$$

and then inserted into Equation 53.

5. NUMERICAL ANALYSIS

The whole numerical analysis has been performed for the three different hatchway covers produced of the three different materials such as polystyrene (E = 3.6 GPa, ν = 0.24, ρ = 1050 kg/m^3), hardened glass (E = 72 GPa, ν = 0.24, ρ = 2900 kg/m^3) and steel (E = 210 GPa, ν = 0.3, ρ = 7850 kg/m^3). While the radius a = 0.3 m and the thickness $h = 6 \bullet 10^{-3}$ m have been assumed to be identical for all the three hatchway covers. Computing the total sound power radiated via the modal analysis requires finding the eigenvalues—the roots of Equation 11—and computing the modal radiation efficiency from Equations 21, 29 and 52, first.

5.1. The Modal Radiation Efficiency

While computing the modal radiation efficiency of mode (m, n), it is worth noticing that this quantity depends on the quotient of the acoustic wavenumber k and the structural wavenumber k_{mn} (cf. Equation 29) and it is independent of all the other geometric and material parameters of the hatchway cover under consideration. Figure 1 shows as the modal radiation efficiency σ_{mn} grows as the parameter k/k_{mn} grows and as approaches values about unity for $k/k_{mn} \geq 1$. The slope of the corresponding curves is relatively small for the small m mode number and for any n mode number. The quantity σ_{mn} approaches values of about 10^{-5} for these mode numbers and $k/k_{mn} = 10^{-1}$. The slope grows considerably as m mode number grows while n mode number stays constant. Figure 1 shows that m mode number influences the slope of σ_{mn} curves much stronger than n mode number. Figure 2 illustrates the absolute approximation error estimated as

$$E_{\text{estim.}} = \left|\sigma_{mn}^{(I)} - \sigma_{mn}^{(A)}\right|, \tag{56}$$

where $\sigma_{mn}^{(1)}$ and $\sigma_{mn}^{(A)}$ are the modal radiation efficiency computed using Equations 21 and 29, respectively. The theoretical value of this error is taken from Equation 29

$$E_{\text{theoret.}} = q_{mn}^2 (k/k_{mn})^8. \tag{57}$$

Figure 2 shows that the estimated error value decreases rapidly as k/k_{mn} decreases. This error assumes values smaller than 10^{-2} for $k/k_{mn} < 0.6$,

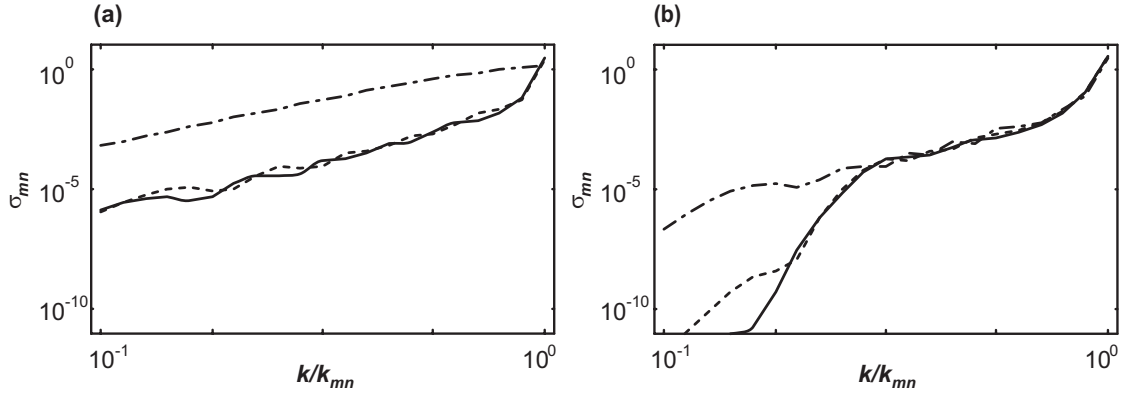

Figure 1. The modal radiation efficiency σ_{mn} for q = 10 and p = 100. *Notes.* –·–·– (a) mode (1,1), (b) mode (2,10); – – – – (a) mode (1,9), (b) mode (10,10); —— (a) mode (1,10), (b) mode (11,10).

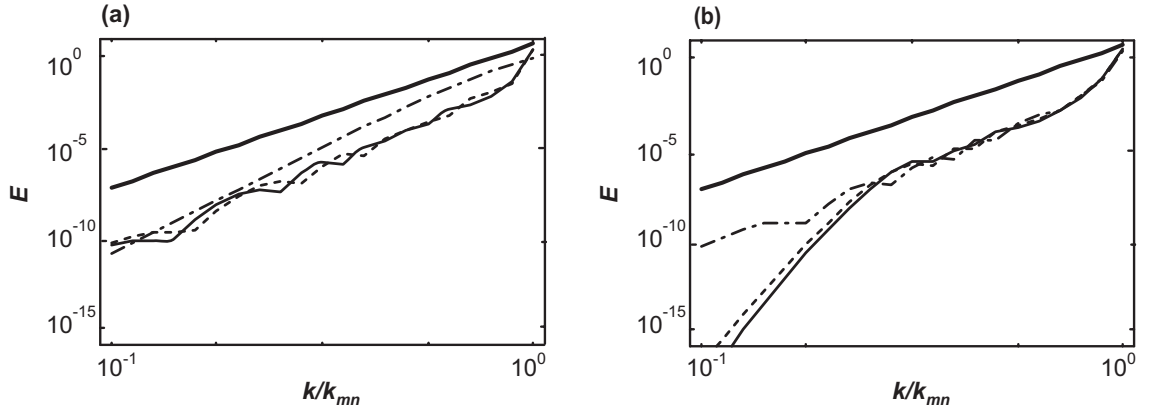

Figure 2. The absolute approximation error *E*: the estimated value (thin lines) and the theoretical value (thick line) for *q* = 10 and *p* = 100. *Notes.* –·–·– (a) mode (1,1), (b) mode (2,10); – – – – (a) mode (1,9), (b) mode (10,10); —— (a) mode (1,10), (b) mode (11,10).

for all modes except for a few where it does not considerably exceed value of for about $k/k_{mn} < 0.2$. Furthermore, the estimated error in Equation 56 does not considerably exceed its theoretical value in Equation 57 for all modes and for $0 \le k/k_{mn} \le 1$. So, Equation 29 gives an acceptable approximation for the radiation efficiency related to the mode (m, n) for $k/k_{mn} < 0.6$ as well as Equation 57 gives a good measure for the corresponding approximation error.

Further, numerical analysis has been performed using Equation 29 for $k/k_{mn} < 0.6$. Figure 3 shows the radiation σ_{mn} as a function of the parameters q

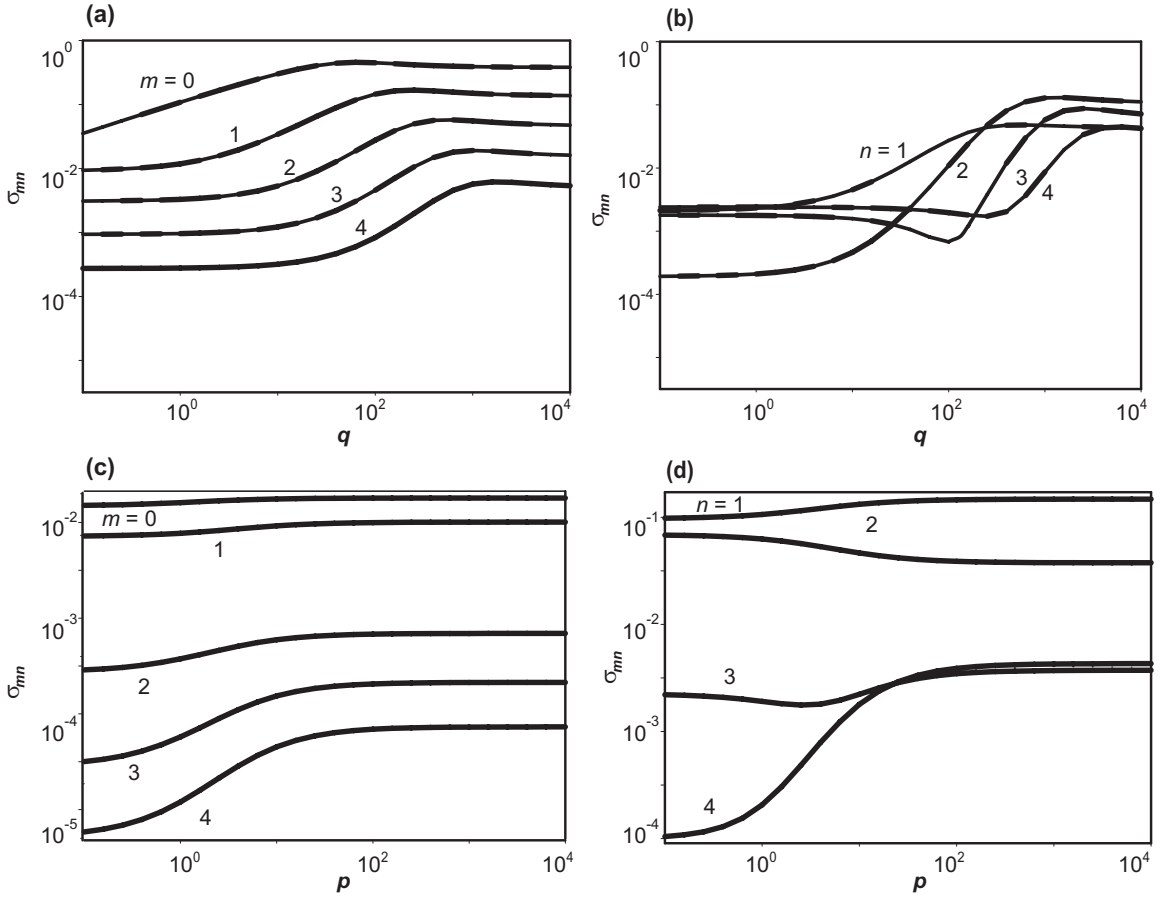

Figure 3. The radiation efficiency σ_{mn} for k/k_{mn} = 0.4: (a) *p* = 100, *n* = 1; (b) *p* = 10, *m* = 2; (c) *q* = 10, *n* = 2; (d) *q* = 100, *m* = 1.

and p for a fixed value of k/k_{mn}. The parameter q strongly influences the radiation efficiency within the range of about $q \in (10^0, 10^4)$ depending on the mode, and weakly outside this range. A decrease in m mode number results in a rapid decrease in the value σ_{mn} (Figure 3a). The radiation efficiency σ_{mn} also strongly depends on the mode number n (Figure 3b). Figures 3c and 3d show that the parameter p strongly influences the radiation efficiency within its range of about $p \in (10^{-1}, 10^2)$ depending on both mode numbers, and weakly outside this range.

5.2. The Total Sound Power

Using the modal analysis for numerical computations of the total acoustic power of the excited plate with any damping neglected requires that the modal radiation efficiency σ_{mn} Equation 21, the intermodal radiation efficiency $\sigma_{mn\ mq}$ Equation 52 and the coefficients $c_{mn}^{(c)}$ and $c_{mn}^{(s)}$ are computed first for a given excitation. The total acoustic power (Equation 51) contains the triple infinite sum. However, this sum must be finite for any numerical computations. This implies that a finite number of modes should be considered giving the following approximation

$$\Pi = \sum_{m=0}^{M}\sum_{n=1}^{N}\sum_{q=1}^{N} \overline{c}_{mn,mq}^{2} \sqrt{\Pi_{mn}^{(\infty)}\Pi_{mq}^{(\infty)}}\,\sigma_{mn,mq} + O[(k/k_{MN})^2], \tag{58}$$

where $(k/k_{MN})^2$ is the theoretical approximation error value. The values M, N have been chosen in such a way that the following conditions is satisfied

$$0 \le k_{\max} \le k_{\mathrm{M-1},\,N-1}, \tag{59}$$

where $k_{\max}$ is the upper bound of the acoustic wavenumber band. The form of Equation 58 implies that the modenumbers M, N should not be too high so that the numerical computation of the triple sum are fast enough. The integrals Equations 21 and 52 contain the troublesome singularities and both are time-consuming. This problem can be overcome by using the fast convergent series 29 instead of the integral 21 for the acoustic wavenumbers $k < k_{mn}$ for the mode (m, n).

The numerical calculations of the total active radiation power have been performed on the basis of Equation 51 where the magnitudes $\sigma_{mn,mq}$ have been obtained from Equations 29 and 52. The modal coefficients $c_{mn}^{(c)}$ and $c_{mn}^{(s)}$ dependent on the material and geometric parameters (mentioned at the beginning of section 5) have been calculated by using Equation 55. The target was to choose the hatchway cover produced of such material that gives the lowest acoustic power level for the arbitrarily chosen amplitude $F_0 = 25\ \pi a^2$ N, $a_0 = 0.15$ m (to assure the asymmetric excitation). Figure 4 shows the sound power level

$$L_{\Pi} = 10\log_{10}(\Pi/\Pi_0), \tag{60}$$

where the sound power is given by Equation 51 and the reference sound power is $\Pi_0 = 10^{-12}$ W. The polystyrene plate generates the sound power level that exceeds 60 dB for $ka \in (1, 6)$, i.e., $f \in (182\ \mathrm{Hz}, 1.09\ \mathrm{Hz})$ since $k = \omega/c$ and $f = \omega/2\pi$, where ω is the excitation frequency, c is the sound velocity in the air). The hardened glass plate is much more silent within this ka range and the corresponding sound power level does not exceed 50 dB. The most silent plate of the three samples is that produced of steel and the corresponding sound power level does not exceed 40 dB within the mentioned ka range. Obviously, all the sample plates generate a considerable sound power level for their resonance frequencies. However, the glass and the steel plates have all their resonances for $ka > 8$ (i.e., $f = 1.45$ kHz). Figure 5 shows the modal contribution level defined as

$$L_{mn} = 10\log_{10}(\overline{c}_{mn}^{2}\Pi_{mn}^{(\infty)}\sigma_{mn}/\Pi_0), \tag{61}$$

where $\overline{c}_{mn}^{2} \equiv \overline{c}_{mn,mn}^{2}$ (cf. Equation 53), $\Pi_{mn}^{(\infty)}$ is given by Equation 20 and σ_{mn} is given by Equations 21 and 29. The greatest contribution of the sample mode (m, n) of the polystyrene plate occurs for k_{mn} be close to k_D, i.e., around the corresponding resonance frequency. It exceeds 50 dB for the mode (0,1) for $ka \in (1,6)$ and for the mode (2,1) for $ka \in (2.5,10)$. This shows that the lowest modes of the sample plate generate some considerable acoustic power levels, and that the polystyrene plate is the most disadvantageous sample of the three sample plates. For given excitation and the geometric parameters it

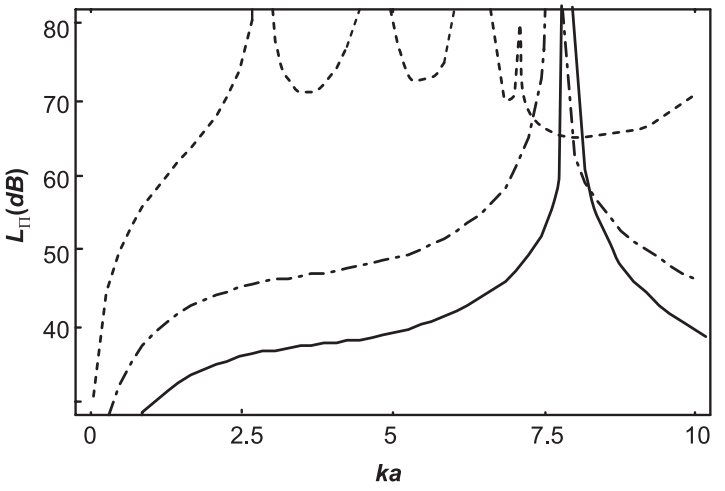

Figure 4. The total sound power level L_Π for some sample hatchway covers. *Notes.* – – – polystyrene, – · – · – glass, —— steel.

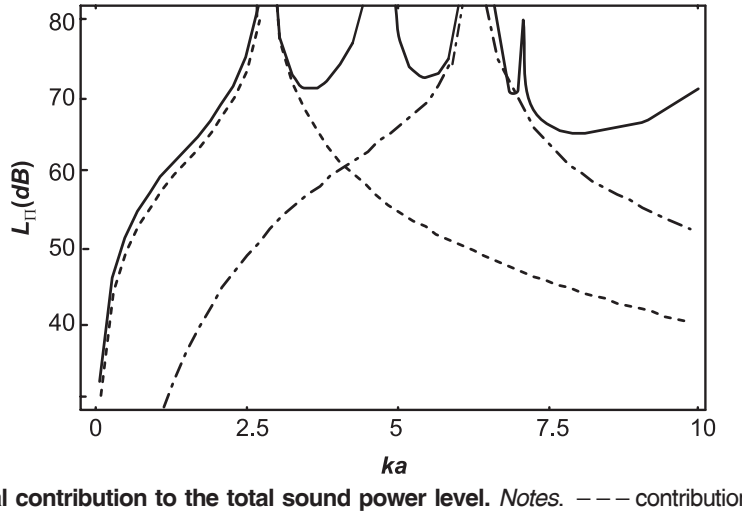

Figure 5. The modal contribution to the total sound power level. *Notes.* – – – contribution of the mode (0,1), – · – · – contribution of the mode (2,1), —— total sound power level.

is necessary to choose a proper material for a hatchway cover to make it acceptably silent.

6. CONCLUDING REMARKS

The low frequency noise of a flat circular plate has been examined using modal analysis. For this purpose, the radiation efficiency of an elastically supported circular plate related to the mode (m, n) has been approximated for the normalized acoustic wavenumber $k/k_{mn} < 0.6$. It has been presented using some developed recurrence formulas. It is a generalization of some earlier published results. First of all, one formula represents the radiation efficiency for the boundary conditions of a clamped circular plate presented earlier [9] as well as for any axisymmetric boundary configuration. Second, results presented earlier [9] were valid for axisymmetric modes only whereas approximation presented herein is valid for both axisymmetric and asymmetric modes.

Equation 29 makes it possible to obtain modal radiation efficiency in a very convenient way avoiding troublesome singularities and integration. Moreover this expression includes only elementary functions, which makes it useful for numerical calculations.

The numerical calculations presented herein have been performed for three different hatchway

covers of identical geometric sizes but produced of three different materials. It has been shown that a circular plate excited asymmetrically by a low frequency concentrated force can generate some considerable sound power levels depending strongly on the plate material parameters. This analysis has made it possible to choose a cover that has the smallest radiation efficiency for a point excitation. However, the formulas presented in this paper can be used to perform a similar numerical analysis for any thin circular plate with any axisymmetric boundary conditions for harmonic excitations.

REFERENCES

1 Czarnecki S, Engel Z, Panuszka Z. Sound power and radiation efficiency of a circular plate. Arch Acoust. 1981;16(4):339–57.

2 Ginsberg JH, Chu P. Asymmetric vibration of a heavily fluid-loaded circular plate using variational principles. J Acoust Soc Am. 1992:91(2): 894–906.

3 Kwak MK, Kim KC. Axisymmetric vibration of circular plates in contact with fluid. J Sound Vib. 1991;146(3):381–9.

4 Amabili M, Frosali G, Kwak MK. Free vibrations of annular plates coupled with fluids. J Sound Vib. 1996:191(5):825–46.

5 Lee H, Singh R. Acoustic radiation from out-of-plane modes of an annular disk using thin and thick plate theories. J Sound Vib. 2005:282;313–39.

6 Levine H, Leppington FG. A note on the acoustic power output of a circular plate. J Sound Vib. 1988;121(2):269–75.

7 Rdzanek Jr WP, Engel Z, Rdzanek W. Theoretical analysis of sound radiation of an elastically supported circular plate. J Sound Vib. 2003;265(1):155–74.

8 Witkowski P. The mutual impedance of two circular plates for high frequency wave radiation. Archives of Acoustics. 1997:22(4):463–72.

9 Rdzanek Jr WP, Rdzanek W. The self power of a clamped circular plate. An analytical estimation. Archives of Acoustics. 2003;28(1):59–66.

10 Meirovitch L. Analytical methods in vibration. New York, NY, USA: MacMillan; 1967.

11 McLachlan NW. Bessel functions for engineers. Oxford, UK: Clarendon Press; 1955.

12 Leissa AW. Vibration of plates, vol. SP-160. Washington, DC, USA: NASA, U.S. Government Printing Office; 1969.

13 Skudrzyk EJ. The foundation of acoustics, basic mathematics & basic acoustics. Vienna, Austria: Springer-Verlag; 1972.

14 Morse PM, Ingard KU. Theoretical acoustics. New York, NY, USA: McGraw-Hill; 1968.

APPENDIX
Developing an Elementary Formula

Equation 21 contains the function $\Psi_{mn}(\theta)$ of an elementary form given in Equation 19. This function has been developed using [11]

$$\int_0^z J_\nu(\xi z)J_\nu(\zeta z)z dz = \frac{z}{\xi^2-\zeta^2}[\xi J_\nu(\zeta z)J_{\nu+1}(\xi z) - \zeta J_\nu(\xi z)J_{\nu+1}(\zeta z)]. \tag{A1}$$

The following substitutions $z = r\big|_0^a$, $\xi = k_{mn}$, $\zeta = k\sin\vartheta$ and $\nu = m$, and denotations from Equation 19 lead to

$$\int_0^a J_m(k_{mn}r)J_m(kr\sin\vartheta)rdr = \frac{a^2}{\lambda_{mn}^2-u^2}[\lambda_{mn}J_{m+1}(\lambda_{mn})J_m(u) - uJ_m(\lambda_{mn})J_{m+1}(u)]. \tag{A2}$$

Substituting, $z = r\big|_0^a$, $\xi = ik_{mn}$, $\zeta = k\sin\vartheta$ and $\nu = m$, and using $I_\nu(z) = \exp(-i\nu\pi/2)\, I_\nu(z\exp(i\nu\pi/2))$ for $-\pi < \arg z \le \pi/2$ [11] lead to $I_m(x) = (-i)^m J_m(ix)$ for $x \in \mathbf{R}$ and give

$$\int_0^a I_m(k_{mn}r)J_m(kr\sin\vartheta)rdr = \frac{a^2}{\lambda_{mn}^2+u^2}[\lambda_{mn}I_{m+1}(\lambda_{mn})J_m(u) + uI_m(\lambda_{mn})J_{m+1}(u)]. \tag{A3}$$

Equations 2 and 19 imply that

$$\begin{aligned} M_{mn}(\vartheta) &= \int_0^a W_{mn}(r)J_m(kr\sin\vartheta)rdr \\ &= A_{mn}\left[\int_0^a J_m(k_{mn}r)J_m(kr\sin\vartheta)rdr + C_{mn}\int_0^a I_m(k_{mn}r)J_m(kr\sin\vartheta)rdr\right]. \end{aligned} \tag{A4}$$

Substituting Equations A2 and A3 into A4 and rearranging the result using denotations from Equation 16 result in the functions $M_{mn}(\theta)$ and and $\varphi_{mn}(\theta)$ as the elementary formulas presented in Equation 19.